Simple Diagnosis of Tropical Cyclone Structure via Pressure Gradients

JOHN A. KNAFF

NOAA/NESDIS/Regional and Mesoscale Meteorology Branch, Fort Collins, Colorado

CHARLES R. SAMPSON

Naval Research Laboratory, Monterey, California

PATRICK J. FITZPATRICK

Geosystems Research Institute, Mississippi State University, Stennis Space Center, Mississippi

YI JIN

Naval Research Laboratory, Monterey, California

CHRISTOPHER M. HILL

Geosystems Research Institute, Mississippi State University, Stennis Space Center, Mississippi

(Manuscript received 1 February 2011, in final form 20 June 2011)

ABSTRACT

In 1980 the Holland tropical cyclone (TC) wind profile model was introduced. This simple model was originally intended to estimate the wind profile based on limited surface pressure information alone. For this reason and its relative simplicity, the model has been used in many practical applications. In this paper the potential of a simplified version of the Holland B parameter, which is related to the shape of the tangential wind profile, is explored as a powerful diagnostic tool for monitoring TC structure. The implementation examined is based on the limited information (maximum wind, central pressure, radius and pressure of the outer closed isobar, radii of operationally important wind radii, etc.) that is typically available in operational models and routine analyses of TC structure. This "simplified Holland *B*" parameter is shown to be sensitive to TC intensity, TC size, and the rate of radial decay of the tangential winds, but relatively insensitive to the radius of maximum winds. A climatology of the simplified Holland *B* parameter based on historical best-track data is also developed and presented, providing the expected natural ranges of variability. The relative simplicity, predictable variability, and desirable properties of the simplified Holland *B* parameter make it ideal for a variety of applications. Examples of how the simplified Holland *B* parameter can be used for improving forecaster guidance, developing TC structure tools, diagnosing TC model output, and understanding and comparing the climatological variations of TC structure are presented.

1. Introduction

There are a number of situations where the diagnosis of tropical cyclone (TC) structure is important. Among these are the quality control of real-time operational analyses (e.g., those produced at the National Hurricane Center), appraisal of TC structure estimate techniques, evaluations of modeled vortex structures and initializations, and studies of tropical cyclone climatologies. However, direct examination of surface winds and pressure gradients within tropical cyclones is often complicated by gaps in vortex information. Among the typically unavailable information is the radius of maximum winds (RMW), which is difficult to diagnose without aircraft-based reconnaissance (Mueller et al. 2006; Knaff and Zehr 2007; Knaff et al. 2007). The reader should note that since U. S. tropical cyclone databases and operational

Corresponding author address: John Knaff, NOAA/NESDIS/RAMMB, Colorado State University, Campus Delivery 1375, Fort Collins, CO 80523-1375.
E-mail: john.knaff@noaa.gov

DOI: 10.1175/WAF-D-11-00013.1

© 2011 American Meteorological Society

forecasts use units of knots (kt, where 1 kt = 0.514 m s^{-1}) for intensity and nautical miles (n mi, where 1 n mi = 1.852 km) for distance, those units will be used throughout this paper.

In this work we propose a simple diagnostic that can be calculated from routinely estimated information including TC vitals, best-track records, TC structure fixes, and routinely available numerical model output. The diagnostic we propose is based upon a simple relationship described in Holland (1980) along with the development of the parametric TC model (H80 hereafter).

Without going into great detail, H80 assumes that TC radial wind (V_c) profiles at the gradient level[1] can be approximated as a family of rectangular hyperbolas in cyclostrophic balance as

$$V_c = (AB\Delta p e^{-A/r^B}/\rho r^B)^{1/2}, \quad (1)$$

where V_c is the cyclostrophic wind as a function of radius, r is the radius, Δp is the pressure difference between the ambient or environmental pressure and the central pressure, e is the base of natural logarithms, ρ is the density of the air, and A and B are scaling parameters. Solving for the radius of maximum wind (i.e., by setting $dV_c/dr = 0$), RMW can be found:

$$\text{RMW} = A^{1/B}. \quad (2)$$

According to Holland (1980), the RMW is independent of the relative values of environmental pressure and central pressure and is defined solely by the scaling parameters A and B. Substituting (2) into (1), an equation for maximum wind ($V_{c\_\max}$, where cyclostrophic balance and no vortex translation are assumed) is obtained by

$$V_{c\_\max} = \left(\frac{B\Delta p}{\rho e}\right)^{1/2}. \quad (3)$$

Rearranging Eq. (3) and assuming ρ is constant yields the relationship between the H80 B parameter and estimates or observations of Δp and V_c (or maximum winds):

$$B = \frac{\rho e V_{c\_\max}^2}{\Delta p}. \quad (4)$$

This relationship is exploited in this paper as a TC diagnostic and the solution of Eq. (4) will be referred to as the "simplified Holland B," or SHB, parameter hereafter. Since the H80 model is derived at gradient level, $V_{c\_\max}$ in (4) is estimated from the storm relative maximum surface wind (V_{srm}) multiplied by a factor of 1.10, and ρ is assumed as to be a constant of 1.2 kg m^{-3} for the calculations shown in the remainder of the paper.

While there are several documented shortcomings of the H80 model, including biases in the height (or pressure) versus wind profile (Willoughby and Rahn 2004) and its overall accuracy of the wind profile (Holland et al. 2010), we are most interested in the SHB parameter as a diagnostic tool—one that is not reliant on measuring the RMW and requires only limited information to calculate. Furthermore, in this work we are not trying to estimate the wind field nor develop the consummate TC structure diagnostic, but rather are asking if the SHB parameter can diagnose TC structure based on readily and routinely available data, namely the maximum wind speed and translation speed (i.e., assuming $V_{c\_\max} \approx V_{\text{srm}}$) and the center-to-environment pressure differences in TCs (Δp). In the following sections it will be shown how Δp and V_{srm} can be estimated from routinely available TC information and how the SHB parameter can serve as a simple diagnostic of TC structure. Specifically, we will demonstrate that structural features can be inferred using the SHB diagnostic. Then, we will show how a climatology of SHB can be constructed using the Atlantic and East Pacific best tracks. Using that climatology, we demonstrate how the SHB may be used in operations to assist in the estimation of TC structural parameters, to appraise satellite-based (and other) TC structure estimates (i.e., fixes), to evaluate model output, and to assess information in best-track files from other basins. Few conclusions regarding differences between models, fixes, and best tracks are presented as they are beyond the scope of this article. In fact, models are treated anonymously throughout the discussions so that the focus remains on the SHB parameter rather than specific model differences.

2. Interpretation of the simplified Holland B parameter

Within this simple framework, Δp represents the difference between central pressure and environmental pressure at some arbitrary radius (r_e) far away from the TC center and thus implicitly is related to TC size. It can also be shown that by assuming cyclostrophic balance (see, e.g., Hess 1959) Δp can be approximated by the integral from the TC center to r_e of the tangential wind (V_t) squared divided by the radius:

[1] For our purposes here, gradient level is the lower level of the free atmosphere where the turbulent stress is negligible and the balance between the pressure gradient and the centrifugal and Coriolis forces (i.e., gradient balance) is an appropriate approximation.

$$\Delta p = -\int_0^{r_e} \rho \frac{V_t^2}{r} dr. \tag{5}$$

This implies that Δp also implicitly includes the effects of the shape and distribution of the azimuthally averaged tangential wind profile. The maximum wind speed is in most cases fairly well related to the radial distribution of the wind field (the winds will decrease inwardly and outwardly from the radius of maximum wind) and thus is simply a proxy for the general and expected shape of the wind profile.

To provide what the SHB parameter may be able to infer about the TC structure, Fig. 1 shows idealized tangential wind profiles constructed with

1) constant maximum surface wind (MSW), RMW, and radius of zero tangential winds, but variable wind profile shapes (cases 1–3);
2) constant MSW, RMW, and wind profile shapes, but with variable radii of zero tangential winds (cases 1, 4, and 5);
3) constant MSW, radii of zero tangential winds, and wind profile shapes, but variable RMW (cases 1, 6, and 7); and
4) constant RMW, radii of zero tangential wind and wind profiles, but variable MSW (cases 1, 8, and 9).

The idealized tangential wind profile is constructed from three pieces and has four free parameters, which are the maximum tangential wind ($V_{\rm tm}$), the exponential decay rate (x), the radius of maximum winds (r_m), and the radius of zero tangential wind (r_o). The first two pieces are a modified rankine vortex where for

$$r \le r_m$$

$$v = v_1 = V_{\rm tm}\left(1 - \frac{r_m}{r}\right), \tag{6a}$$

and for $r_m > r \ge 2r_m$

$$v = v_2 = V_{\rm tm}\left(\frac{r_m}{r}\right)^x. \tag{6b}$$

The third piece of the profile is a weighted average of v_2 (the rankine vortex outside the RMW) and v_3 (a linear decrease of tangential wind with radius outside twice the RMW) defined as

$$v_3 = V_{\rm tm}\left(\frac{r_m}{2r_m}\right)\left[1 - \frac{(r - 2r_m)}{(r_0 - 2r_m)}\right], \tag{6c}$$

so that for $2r_m > r \ge r_0$,

$$V_t = w_2 v_2 + w_3 v_3, \tag{6d}$$

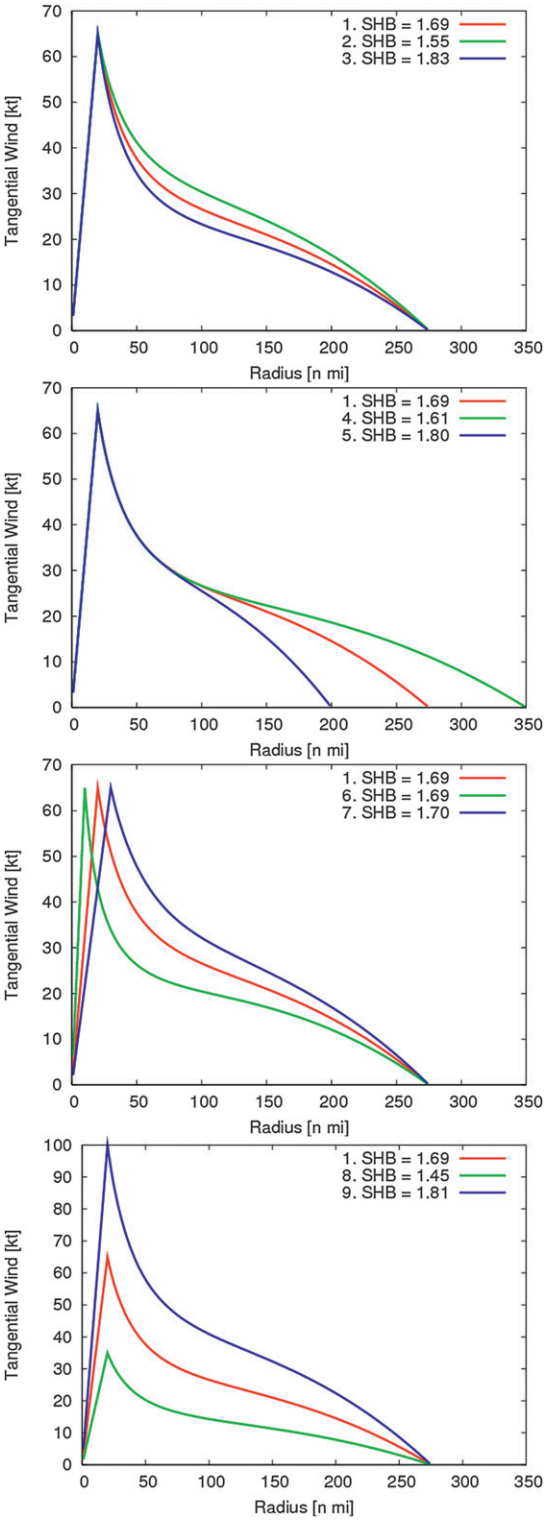

FIG. 1. Idealized tangential wind profiles and their corresponding SHB parameters. The first through fourth panels explore sensitivities of the SHB parameter to the wind profile shape, radius of zero tangential winds, radius of maximum wind, and maximum wind speed, respectively. The full details of the experiments can be found in Table 1.

TABLE 1. Details of the idealized tangential wind profile cases including vortex parameters (r_m, x, V_{tm}, r_0) and results in terms of pressure deficit (Δp) and the SHB parameter.

Case	r_m (n mi)	x	V_{tm} (kt)	r_0 (n mi)	Δp (hPa)	SHB
1	20	0.6	65	275	−26.1	1.69
2	20	0.5	65	275	−28.4	1.55
3	20	0.7	65	275	−24.1	1.83
4	20	0.6	65	350	−27.3	1.61
5	30	0.6	65	200	−24.5	1.80
6	10	0.6	65	275	−26.1	1.69
7	30	0.6	65	275	−25.9	1.70
8	20	0.6	35	275	−8.8	1.45
9	20	0.6	100	275	−57.7	1.81

where

$$w_2 = 1 - w_3$$
$$w_3 = \frac{(r - 2r_m)}{(r_0 - 2r_m)}.$$

Finally, at radii greater than r_0, $V_t = 0$.

Table 1 provides the case number that corresponds to the profiles shown in Fig. 1, the parameters used to create each tangential wind profile, the resulting Δp, and the SHB parameter produced by each case. For our purposes here, Δp is calculated from azimuthally averaged gradient winds and by integrating inward from the radius of zero tangential wind. Surface winds are increased by a factor of 1.1 and ρ is assumed to be equal to 1.2 kg m^{-3} and all calculations are done at 25° latitude.

The top panel in Fig. 1 shows vortices that have the same size (i.e., r_o), RMW, and MSW, but the x parameter is variable. The SHB parameter calculated using Eq. (4) increases with increasing x parameter, implying that more compact TC vortices have larger SHB values. The second panel in Fig. 1 shows a set of SHB values derived from changing the size of the vortex by increasing and decreasing r_0. This panel shows that SHB is inversely proportional to the vortex size. The third panel in Fig. 1 shows the SHB sensitivities to variations in RMW. Of note is that the SHB parameter appears to be insensitive to variations in RMW, at least for this limited set of TC-like vortices. Finally, the bottom panel in Fig. 1 shows the SHB sensitivity to MSW, and as may be expected from Eq. (4), the SHB parameter is correlated with MSW. To summarize, higher (lower) values of the SHB parameter are associated with vortices with compact (broad) tangential wind profiles and intense (weaker) maximum tangential winds. Finally, the SHB parameter appears to be insensitive to changes in RMW when other factors are held constant.

The SHB parameter thus appears to be a useful TC diagnostic especially when the details of the wind profile and pressure gradient are limited, as is commonly the case. In fact, routine operational tracks, year-end best tracks, and numerical model output (i.e., tracker output) typically include enough information to estimate the SHB parameter. We also know that the SHB parameter theoretically ranges between a value of 1.0 and 2.5, as discussed in Holland (1980), but if SHB is going to be useful as a TC diagnostic, we are more interested in the climatological ranges of SHB. To explore this issue, the next section calculates the SHB parameter based on existing best-track information, providing the natural ranges of SHB.

3. Climatology of the simplified Holland *B* parameter

To show how the SHB parameter likely varies in nature and between basins, the SHB is estimated from the information available in the Atlantic and eastern Pacific best-track data available in the Automated Tropical Cyclone Forecast system (ATCF; Sampson and Schrader 2000). To estimate the SHB parameter, the Courtney and Knaff (2009, herafter CK09) wind–pressure relationship algorithm is used to estimate a central pressure and Δp as a function of latitude, MSW, translation, environmental pressure (EP), and size (radius of gales). For these calculations EP can be derived from the pressure of the outermost closed isobar (POCI) information available in the working and final best tracks using EP = POCI + 2 hPa. More details on the CK09 algorithm and how these parameters can be estimated using routinely available best-track information are provided in the appendix.

The storm-relative maximum surface wind [i.e., V_{srm}; see (A1), and (A2)] is calculated by subtracting the Schwerdt et al. (1979) asymmetry factor ($1.5c^{0.63}$, where c is the translation speed in kt) from the MSW. For our purposes, c is estimated from the 6-hourly best-track TC positions of tropical systems. Using these best-track estimates of V_{srm} and Δp, the SHB parameter is estimated using Eq. (4), noting again that the maximum cyclostrophic gradient-level wind is estimated by $V_{c\_max} = 1.1V_{srm}$. The results for the 2003–09 Atlantic and east Pacific best tracks are shown in Fig. 2.

In terms of the SHB parameter there is greater variability in the Atlantic basin than in the east Pacific basin. These differences can be explained by differences between the two regions' climatologies. TCs in the eastern Pacific are generally smaller (Knaff et al. 2007, 2010), have a smaller range of latitudes, and tend to have slower mean motions (Neumann 1993) than those in the Atlantic. In addition to the smaller sizes, storms in the east Pacific usually move westward their entire lives and rarely recurve into the midlatitudes (Neumann 1993; Blake et al. 2009). In the Atlantic, storms do gain latitude

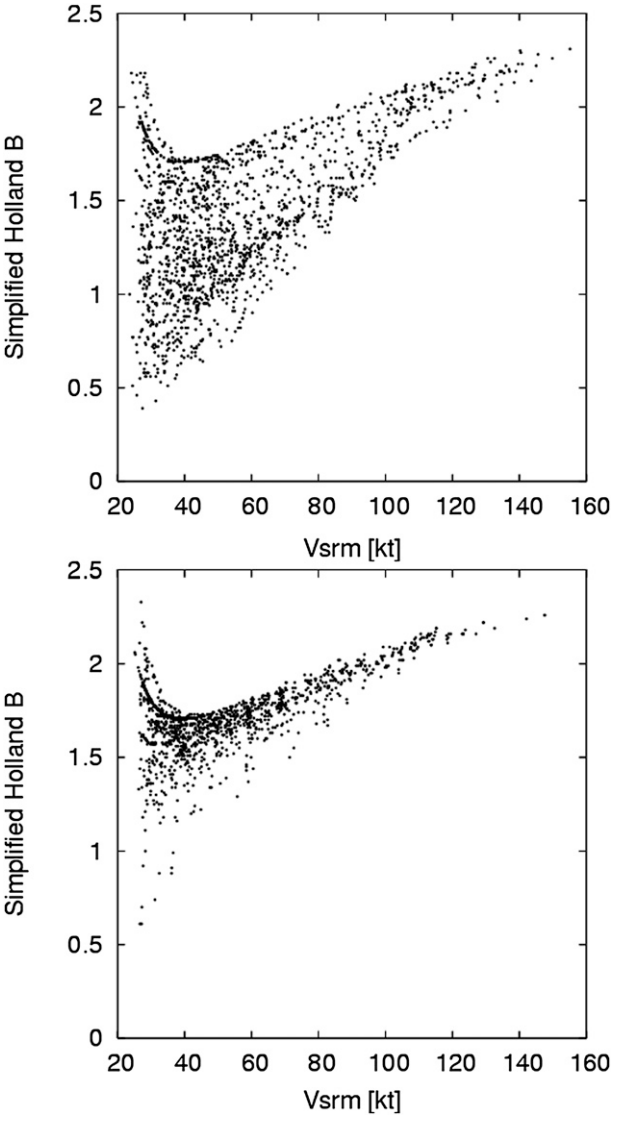

FIG. 2. The SHB distribution as a function of storm-relative maximum surface winds (V_{srm}) for the (top) North Atlantic and (bottom) eastern Pacific based on 2003–09 best-track data. The North Atlantic and eastern Pacific have 1671 and 1379 cases, respectively.

and can maintain high intensities even after recurvature (Knaff 2009). Storms also tend to grow and weaken as they move poleward (Merrill 1984; Knaff et al. 2007; Vickery and Wadhera 2008). TCs also are prone to growth even while intensifying during interaction with moderate vertical wind shear, which ismost common at the higher latitudes (Maclay et al. 2008). The climatological distributions shown here contain key information regarding both the observed bounds of the SHB parameter with respect to intensity, and some basic interbasin climatological differences. Such information will be exploited in the next section, which discusses potential applications of the SHB parameter.

4. Applications of simplified Holland *B* parameter

a. Operational TC vitals guidance

At the U.S. warning centers an estimate of the "TC vitals"[2] is created in the first hour of the forecast process, which starts at the synoptic hours of 0000, 0600, 1200, and 1800 UTC and ends 3 h later when TC advisories are issued [see Rappaport et al. (2009) for products at the National Hurricane Center]. The TC vitals include information about maximum surface wind, location, and operationally important wind radii. Estimates of these operationally important wind radii are often less certain than estimates of other parameters (Knaff et al. 2010). With the SHB ranges shown in Fig. 1, an interactive forecaster dialog could be developed that notifies the forecaster when the information in the TC vitals produces SHB values outside observed ranges (Fig. 2) and returns additional feedback to the forecaster. For instance if a set of wind radii result in relatively large values (versus climatology) of SHB, the feedback could be a statement that "the information you have provided for the TC vitals produced SHB values indicative of a small tropical cyclone" or from a SHB climatology could suggest what are reasonable values of the radii of 34-kt winds (R34) that correspond to small, average, and large TCs for a given intensity estimate.

A diagnostic tool, as was described above, could be developed to work within current operational platforms. This very simple diagnostic, by providing very simple feedback on estimated structure parameters (i.e., wind radii), will likely lead to more consistent and realistic TC structure estimates in the TC vitals. Presumably, if the TC vitals are used for model initialization, these improved estimates should then result in improved track and intensity forecasts. Finally, improved TC structure information provided in real time influences the postseason best tracks, so these diagnostic results could also influence tropical cyclone climatologies. This application of SHB would be most useful for training and for forecasters making estimates of TC structure when the observations are contradictory or inadequate.

b. Examination of satellite-based (or other) TC structure estimates

Another potential diagnostic application of the SHB parameter is in the evaluation of TC structure estimates.

[2] The TC vitals are subjectively derived analyses of the TC locations, intensities, and structures. While subjective, these are real and useful estimates of the TC structures, intensities, and locations, which are based on the available observations. Unfortunately, in past work these analyses have been referred to as "the bogus"—a name that is unrepresentative of their true nature. These estimates are provided in the CARQ lines of the ATCF's a-deck databases.

Here, we provide an example of satellite-based estimates of the surface wind field from the Multiplatform Tropical Cyclone Surface Wind Analysis (MTCSWA; Knaff et al. 2011, hereafter KDMSS), which creates a surface wind analysis from four satellite-based surface and near-surface wind field estimates. The inputs come from nonlinear balance winds calculated from the Advanced Microwave Sounding Unit (AMSU; Bessho et al. 2006), operational cloud drift feature track winds (CDFTs; Holmlund et al. 2001), and water vapor feature track winds (WVs; Velden et al. 1997) from geostationary satellites, infrared flight-level analog winds (IRWDs; Mueller et al. 2006), and scatterometery (SCAT; Gelsthorpe et al. 2000; Graf et al. 1998). Without going into great detail, the MTCSWA optimally combines winds from these disparate sources to estimate a grid of 10-m winds with generally lower RMS errors than the individual sources. However, that does not mean the analysis compensates for all of the errors in the input. Specifically, AMSU winds are hindered by the 50-km resolution of the instrument, SCAT wind speeds saturate as they approach hurricane force, and near-surface CDFT and WV winds are rarely available near the centers of TCs. Finally, the IRWD is based on a rankine vortex, and is known to have a high bias for small (less than 20 km) RMWs (Mueller et al. 2006; Knaff et al. 2007). Not surprisingly, the MTCSWA also has its largest errors in the vicinity of the RMW, and the analysis biases suggest that the RMW is often too large (KDMSS).

The simplified Holland B parameter calculated from MTCSWA output as a function of V_{srm} is shown in Fig. 3 for the Atlantic (top) and east Pacific (bottom). Also shown are the approximate upper and lower bounds of the SHB parameter from Fig. 2. A quick look at Fig. 3 suggests that the SHB diagnostic calculated from MTCSWA is primarily in the climatological ranges until V_{srm} approaches ~90 kt and that above this intensity the SHB has a low bias. This outcome, based simply on SHB, implies that the wind field is generally too broad for TCs with intensities greater than ~100 kt. This quick conclusion is nonetheless consistent with our knowledge of the known shortcomings of the MTCSWA. The verification statistics based on a comparison of MTCSWA and H*WIND analyses (Powell et al. 1998), which contain aircraft-based observations, indeed show that MTCSWA has a tendency to overestimate winds within 100 km of the TC center. Similar comparisons with best-track hurricane force (64 kt) wind radii showed that MTCSWA also generally overestimates the extent of hurricane force (64 kt) winds (KDMSS).

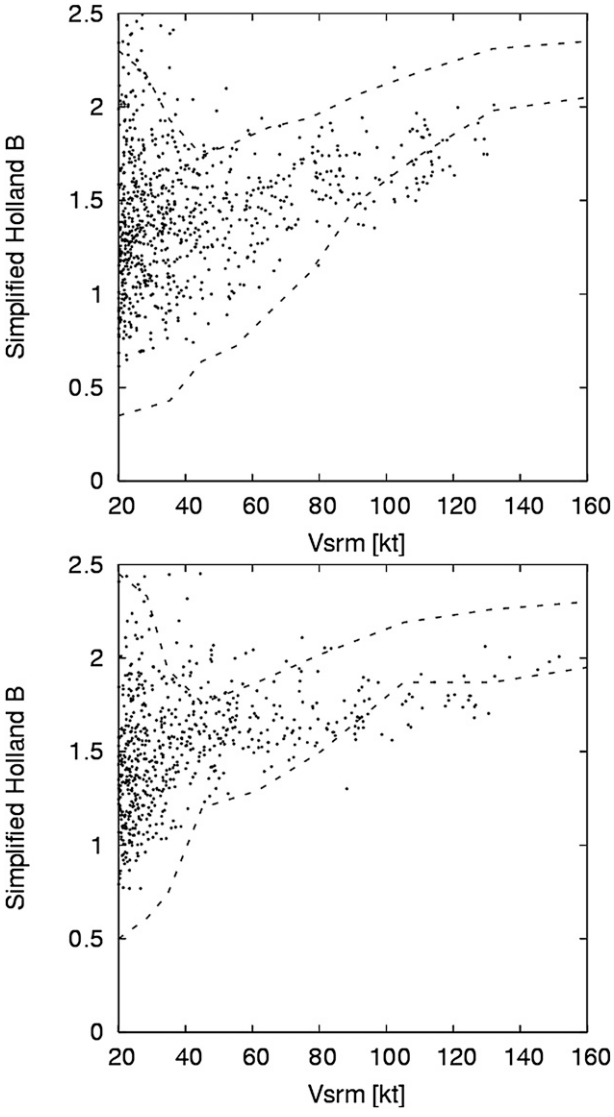

FIG. 3. SHB parameters calculated from the 2009–10 MTCSWA wind field estimates as a function of V_{srm} for the (top) Atlantic and (bottom) eastern Pacific, which has 1272 and 861 cases, respectively. Dashed lines provided estimates maximum and minimum SHB bounds from Fig. 2.

c. Model diagnosis of TC structure

Just as the SHB parameter can be used to provide guidance for the TC vitals, details concerning how the initial SHB parameter compares with the TC vitals observations and how the SHB parameter evolves during forecasts can be elucidated. Furthermore, since the SHB parameter is relatively insensitive to variations of the RMW, models with similar resolutions can be easily compared using this diagnostic. The diagnostic can be used to assess how well the model compares with the best-track values, how the initialization compares with the TC vitals, and whether the inferred tangential wind profiles evolve in a reasonable or anticipated manner.

Examples of how the SHB parameter could be used to diagnose issues with the initialization of hurricane models are shown in Fig. 4, which compares the SHB associated

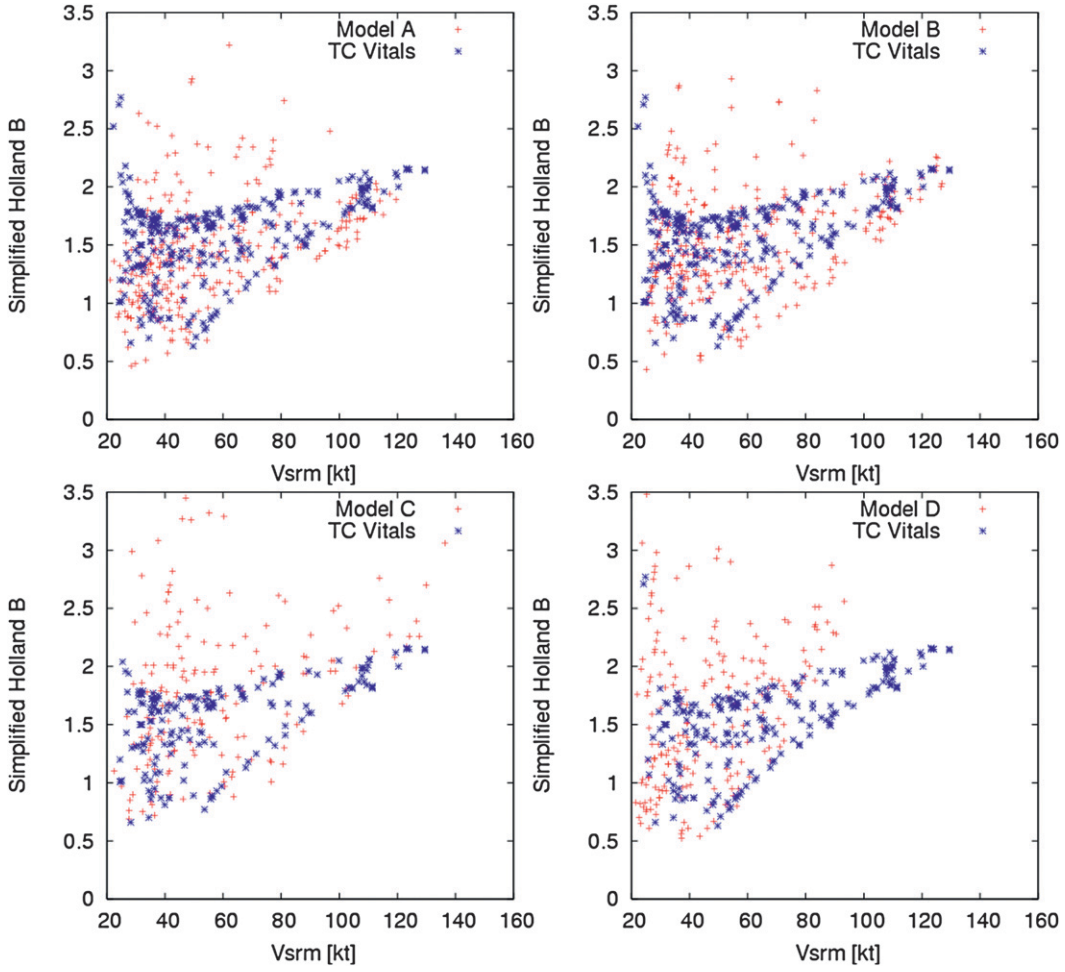

FIG. 4. SHB values as a function of V_{srm} for the initial TC vitals (blue asterisk) and for model initial conditions (red crosses). Results are shown for models (top left) A, (top right) B, (bottom left) C, and (bottom right) D, which have 300, 305, 188 and 210 cases, respectively. See text for further descriptions of these comparisons.

with the TC vitals to those of three hurricane models (models A–C) and one global model (model D) at $t = 0$ for all the valid Atlantic forecasts made during 2010. The horizontal resolutions of models A–C are comparable, ranging from 5 to 10 km, while model D has a resolution around 27 km. To calculate the SHB values in Fig. 4, we used 1) the TC vitals observations to obtain the initial 6-hourly motion, MSW, latitude, nonzero average radius of 34-kt winds (R34), and the POCI (to estimate EP) at the initial times, and 2) the model's initial MSW, central pressure, and latitude, as well as the forecasted 6-hourly translation speed. Model forecasts of Δp are calculated using the best-track POCI (to estimate EP) and the models' forecasts of central pressure. For the remainder of the discussion we will just call these models A, B, C, and D, since the purpose of this paper is to introduce the SHB parameter as a TC diagnostic and not to perform extensive model evaluation.

In Fig. 4 the asterisks are the SHB parameter based on TC vitals at $t = 0$ and the crosses are the initial conditions of models A (top left), B (top right), C (bottom left), and D (bottom right). A large disparity is seen in the initial structures between the numerical models and the observations (i.e., the TC vitals). In all of the models there are a number of values of SHB that are outside the observed ranges (Fig. 2) and that are quite different than the TC vitals would indicate they should be. Model D, the global model, shows its inability, due to resolution constraints, to be initialized with intensities much greater than 85 kt. As a result, it appears that the more intense storms in model D are represented by relatively large values of the SHB parameter when compared to the initial conditions of mesoscale hurricane models, suggesting that the intensities provided by the model are too large given the CP and/or the radial decrease in tangential wind is unrealistically large. At any rate, one can quickly conclude that

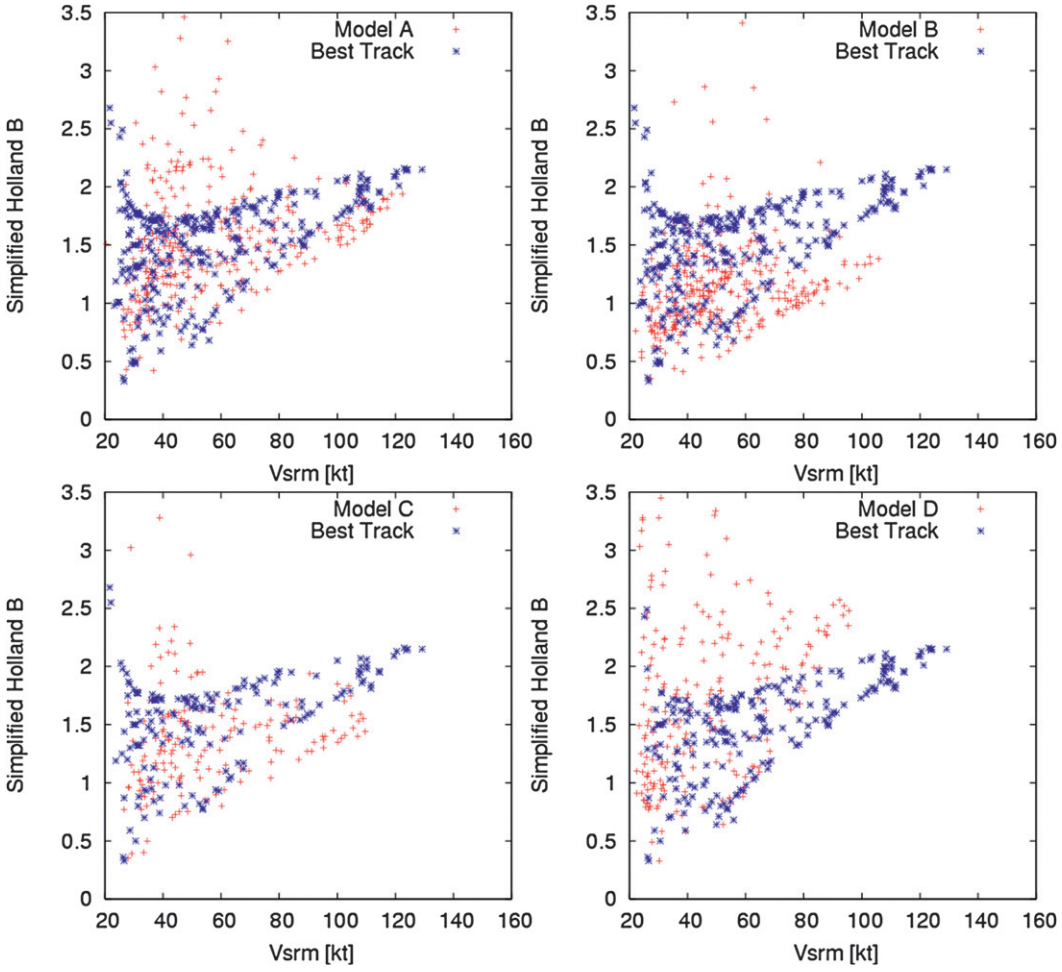

FIG. 5. Same as Fig. 4 but for the valid best-track time (blue asterisk) and for model 12-h forecasts (red crosses).

the vortex in this global model is much different than the vortex in nature, which is not all that surprising given the resolution of this global model. It is also curious however that in the intensity ranges where this high SHB bias occurs in models A–C (i.e., 25–80 kt), operationally important wind radii are not always available in the TC vitals for each quadrant. For instance, an average of 34-kt wind radii, which includes zero values, would result in a smaller storm and higher values of the SHB parameter. This speculation gives model developers a working hypothesis for what may be causing these differences. For the more intense TCs, model A seems to be biased toward low SHB (i.e., inferring broader tangential wind profile). Model B has a similar tendency. Model C, on the other hand, generally looks high biased for higher intensities. This suggests that model A, which appears to do a good job of initializing weaker storms, has a tendency to initialize broader wind profiles than observed for more intense storms. This issue may solely be a result of resolution and could lead researchers to test initialization sensitivities to resolution to confirm or deny this suspicion.

In addition to the initialization, how the SHB parameter changes from the initial conditions may also be of interest. Figure 5 shows the 12-h forecasts for the same set of storms whose initialization is shown in Fig. 4 along with the operational best-track values of the SHB parameter valid at the 12-h forecast time. These forecasts displayed have not been ''interpolated,'' which is a common operational practice and is discussed in Sampson et al. (2006, 2008) and Goerss et al. (2004). In this case the asterisks represent the best-track SHB parameter valid at the time of the forecast. In comparing Figs. 4 and 5, notice how quickly the initial SHB conditions change, particularly in model B and to a lesser extent in model C. All models appear to have lower intensities (i.e., maximum winds) than observed, which would lead to smaller values of SHB (see section 2). Model A has a tendency toward both decreasing the SHB parameter for forecast intensities above 60 kt and increasing the SHB parameter for storms

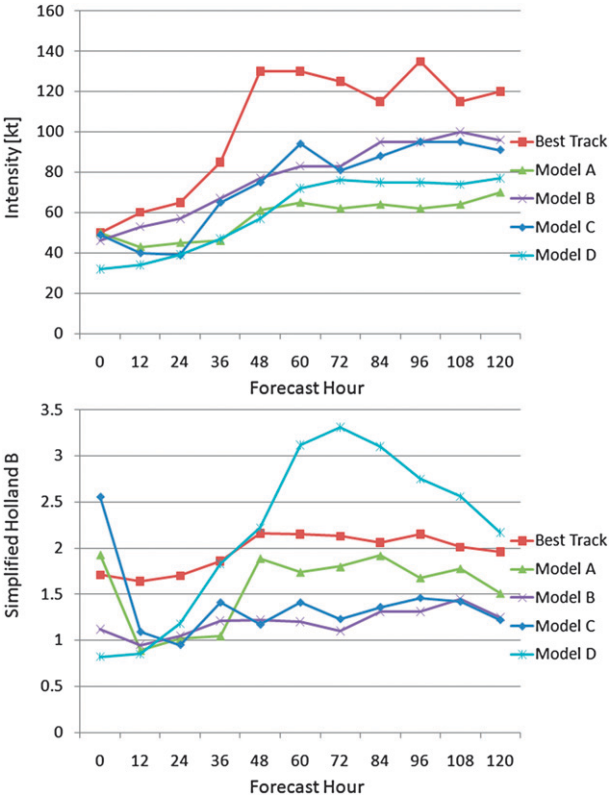

FIG. 6. Typical TC model forecasts in terms of (top) MSW and (bottom) SHB parameters during a period of rapid intensification.

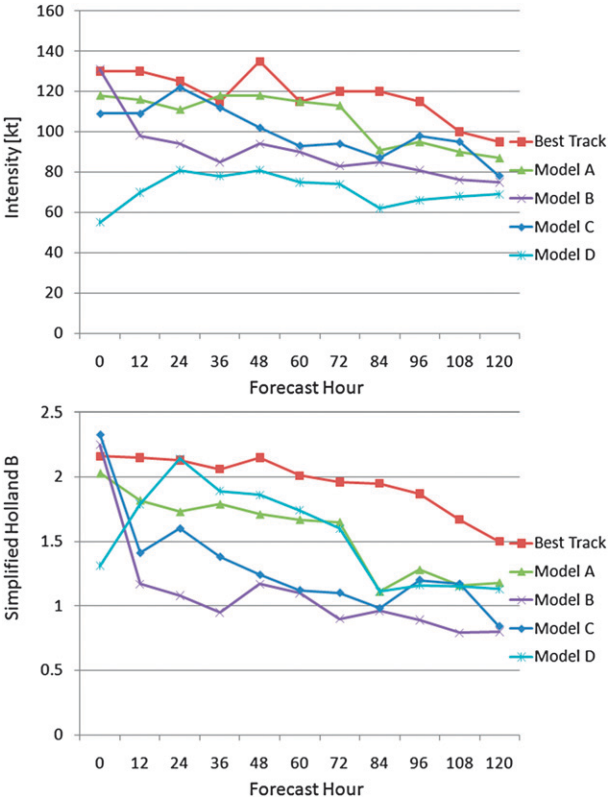

FIG. 7. Same as Fig. 6 but during a period of steady or weakening intensities.

with intensities below 60 kt. Model B tends toward lower SHB values and has a pronounced low intensity bias. Model C also decreases the SHB parameter and intensities, but to a lesser extent. The 12-h SHB distributions seem to be fairly close to the climatological distributions for both models A and C. Model D is nearly unchanged with a slight tendency to increase the SHB parameter (inferring a tightening of the wind profile). While intensity biases are routinely monitored, the SHB parameter can show additional TC structure tendencies, and shortcomings.

While Figs. 4 and 5 provide a general picture of how well the initial vortices fit within the observation space and how the model TC structure changes in the first 12 h of integration, respectively, specific forecasts can also be examined, as shown in Figs. 6 (a rapid intensification case) and 7 (a steady and weakening case). The intensity forecast comparisons are shown in the top panel while the SHB forecast comparisons are shown in the bottom panel for both figures. Figure 6 shows a typical rapid intensification case where the TC increases from 65 to 130 kt between the 24- and 48-h forecasts. In the top panel it is clear that all of the models have difficulty predicting a rapid intensification event. Models A and C both suffer some structural changes in the early stages of the forecast (bottom panel), though those changes are not as evident in the intensity trends (top panel). Modelers have communicated that mesoscale models that use the TC vitals in their initialization (as both of these models do) can experience an imbalance in the initial stages of a forecast. The global model (model D) demonstrates low intensities throughout the forecast, but the SHB values get very large (unrealistically large) by 72 h. From Eq. (4), it appears that the pressure gradient may be unrealistically small for the forecast intensity. Models B and C settle into a rather narrow range of SHB values throughout the forecast, even while the storm is intensifying (i.e., SHB should be increasing).

Figure 7, on the other hand, demonstrates model forecasts during more steady intensity conditions that are followed by weakening. In this case the observations show that the SHB parameter becomes smaller as the storm weakens. Model A's forecast of intensity is low biased, but its trends follow the observations. Model B shows a rapid weakening in the first 12 h, followed by a trend that closely matches the observations in time. In terms of the SHB parameter, all models have low biases, indicating that the distribution of pressure for the given intensity is different than in nature; in this case we can infer that the tangential wind profile is broader than is

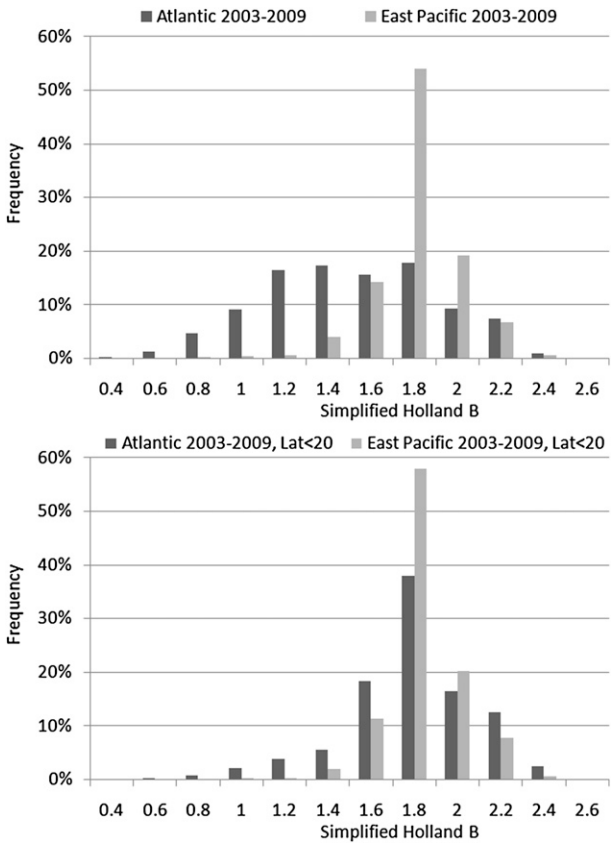

FIG. 8. (top) Frequency distributions of the SHB parameter for the Atlantic and eastern Pacific TC basins during 2003–09 and (bottom) the same analysis but constrained to TCs equatorward of 20°N. There are 1671 and 1379 cases for the Atlantic and East Pacific, respectively, used in the top panel and 533 and 1157 cases used in those basins in the bottom panel.

typically observed in nature. Models A–C show a tendency for the SHB parameter to decrease during its period of nearly constant intensity, which is expected as this storm is moving poleward. Model D's SHB increases from the initialization during the first 24 h and then starts a steady decrease like the other models. It is also noteworthy that while the discussion in section 2 (and the best-track V_{max} versus SHB shown in Figs. 6 and 7) implies that the SHB parameter is fundamentally correlated with intensity, one would not easily conclude this from the model forecasts of SHB shown in Figs. 6 and 7.

d. Best-track comparisons

The SHB information shown in Fig. 2 can also be displayed in terms of a frequency distribution, as shown in the top panel of Fig. 8. In this case one can see that 1) the Atlantic basin has greater variability in SHB than does the eastern Pacific basin, 2) storms in the Atlantic tend to have broader wind profiles (and lower SHB values) than their east Pacific counterparts, and 3) the frequency of high values of SHB is much greater in the eastern Pacific, where there are generally more compact storms. These basin-to-basin differences suggest that the TC structures in the North Atlantic are quite different than they are in the east Pacific; however, when we consider only TCs that were located equatorward of 20°N in both basins, the distributions appear more similar (Fig. 8, bottom). The Atlantic storms are still more variable in terms of SHB, implying that less compact storms occasionally can occur in the low-latitude Atlantic. While beyond the scope of this paper, the SHB parameter could be calculated from global best-track datasets. Such analyses would be useful for engineering applications (e.g., Vickery and Wadhera 2008) or for comparing analyses from different agencies—a task particularly relevant to future efforts like the International Best Tracks Archive for Data Stewardship (Knapp et al. 2010).

5. Summary

A simplified Holland *B* (SHB) parameter, shown in (4), is introduced as a TC structure diagnostic. While the SHB parameter is not the consummate TC structure diagnostic, it has several desirable qualities including its relative insensitivity to the RMW, its easy calculation from routinely available information contained in model output and historical datasets, and its straightforward representation of many aspects of TC structure as a single parameter.

These qualities make the SHB parameter useful for a number of diagnostic applications. In operations, such diagnostics could help forecasters to quality control wind radii for the forecast advisory and the TC vitals. the SHB parameter also allows for quick and easy diagnoses of model TC structure. This could be particularly useful in the National Oceanic and Atmospheric Administration's Hurricane Forecast Improvement Project, which is designed to improve hurricane forecasts over a 10-yr period and which strongly emphasizes the improvement of NWP models. The SHB parameter can also aid in the development of satellite-based pressure and related wind estimates where the horizontal instrument resolution is limited and/or variable (e.g., satellite sounder data). The SHB parameter could also be used for historical data comparisons and climatological studies focused on tropical cyclone size, structure, and intensity. And, finally, the SHB parameter may provide value in comparing basin-to-basin and interagency best-track information. The list provided above is not meant to be comprehensive, but we feel the meteorological community should at least be aware of these SHB applications.

Acknowledgments. This project is supported by the NOAA Hurricane Forecast Improvement Project (NA09AANWG0149) and the Northern Gulf Institute

(NA06OAR4320264), as well as by the U.S. Department of Homeland Security under Award 2008-ST-061-ND 0001. The authors would also like to thank the two anonymous reviewers, Mark DeMaria, Andrea Schumacher, and Mike Fiorino for providing constructive comments on the many versions of this manuscript. The views, opinions, and findings contained in this report are those of the authors and should not be construed as an official National Oceanic and Atmospheric Administration or U.S. government position, policy, or decision.

APPENDIX

The Courtney and Knaff (2009) Wind–Pressure Relationship

As a review, Courtney and Knaff (2009) adapted the results of Knaff and Zehr (2007, hereafter KZ07), which related the MSW to Δp as a function of latitude, translation speed, TC size, and EP, by 1) making estimates of EP and TC size using routinely available (in operations) information and 2) modifying the original KZ07 formula for storms located at low latitudes. Instead of using global analysis fields as proposed in KZ07, CK09 used R34 to estimate TC size and POCI is used to estimate of EP.

The Δp can be estimated given the latitude φ.

For $\varphi < 18°$,

$$\Delta p = 5.962 - 0.267V_{\text{srm}} - \left(\frac{V_{\text{srm}}}{18.26}\right)^2 - 6.8S. \quad \text{(A1)}$$

For $\varphi \geq 18°$,

$$\Delta p = 23.286 - 0.483V_{\text{srm}} - \left(\frac{V_{\text{srm}}}{24.254}\right)^2 - 12.587S - 0.483\varphi, \quad \text{(A2)}$$

where V_{srm} is the storm-relative MSW in knots defined by $V_{\text{srm}} = \text{MSW} - 1.5c^{0.63}$ [i.e., the Schwerdt et al. (1979) asymmetry factor], where c is the translation speed of the TC in knots, S is a TC size parameter, and φ is measured in degrees latitude. Here, S is defined as the ratio of the azimuthal mean tangential wind at $r = 500$ km (V_{t500}) to the climatological value (V_{t500c}) in knots (A3). In CK09, the V_{t500} is estimated directly from the nonzero quadrant average of the radii of 34-kt winds (R34_{avg}), where $V_{t500} = (\text{R34}_{\text{avg}}/9) - 3$, also in knots. CK09 applied a lower limit to S of 0.4 to ensure operational stability; here, we will limit S calculated in this manner to 0.1, roughly within two standard deviations of the KZ07 observations, allowing for very small TCs. From the Atlantic basin climatology developed in Knaff et al. (2007), we define V_{t500c}:

$$V_{t500c} = \text{MSW}\left\{\frac{[66.785 - 0.091\,02\text{MSW} + 1.0619(\varphi - 25)]}{500}\right\}^{[0.1147 + 0.0055\text{MSW} - 0.001(\varphi - 25)]}. \quad \text{(A3)}$$

For the CP estimates it should be noted that we linearly weight the Δp calculated by (A1) for latitudes less than 18° and (A2) between the latitudes of 18° and 25°.

Since POCI, MSW, φ, c, and R34 are routinely available in the databases of the ATCF (Sampson and Schrader 2000), CP and Δp can be calculated, where CP = Δp + POCI + 2 (hPa). Sensitivity to the individual parameters is discussed in terms of composites in Knaff and Zehr (2007) and a table is provided in Knaff and Harper (2010). The method has been shown to outperform standard pressure–wind relationships from Dvorak (1984) and the results suggest that the method can explain 90%–95% of the variability when compared to aircraft-based CP results and corresponding best-track maximum wind speeds (see Knaff and Harper 2010; KZ07).

REFERENCES

Bessho, K., M. DeMaria, and J. A. Knaff, 2006: Tropical cyclone wind retrievals from the Advanced Microwave Sounder Unit (AMSU): Application to surface wind analysis. *J. Climate Appl. Meteor.,* **45,** 399–415.

Blake, E. B., E. J. Gibney, D. P. Brown, M. Mainelli, J. L. Franklin, T. B. Kimberlain, and G. R. Hammer, 2009: *Tropical Cyclones of the Eastern North Pacific Ocean, 1949-2006*. Historical Climatology Series, Vol. 6-5, National Climatic Data Center, 166 pp. [Available on-line at http://ols.nndc.noaa.gov/plolstore/plsql/olstore.prodspecific?prodnum=C00755-PUB-A0001.]

Courtney, J., and J. A. Knaff, 2009: Adapting the Knaff and Zehr wind–pressure relationship for operational use in tropical cyclone warning centres. *Aust. Meteor. Oceanogr. J.,* **58,** 167–179.

Dvorak, V. F., 1984: Tropical cyclone intensity analysis using satellite data. NOAA Tech. Rep. 11, 45 pp. [Available from NOAA/NESDIS, 5200 Auth Rd., Washington, DC 20333.]

Gelsthorpe, R. V., E. Schied, and J. J. W. Wilson, 2000: ASCAT—MetOp's advanced scatterometer. *ESA Bull.,* **102,** 19–27.

Goerss, J. S., C. R. Sampson, and J. M. Gross, 2004: A history of western North Pacific tropical cyclone track forecast skill. *Wea. Forecasting,* **19,** 633–638.

Graf, J. E., W.-Y. Tsi, and L. Jones, 1998: Overview of QuikSCAT mission—A quick deployment of a high resolution, wide swath scanning scatterometer for ocean wind measurement. *Proc. IEEE Southeastcon '98: Engineering for a New Era,* Orlando, FL, IEEE, 314–317. [Available online at http://ieeexplore.ieee.org/xpls/abs_all.jsp?arnumber=673359.]

Hess, S. L., 1959: *Introduction to Theoretical Meteorology*. Robert E. Krieger Publishing, 362 pp.

Holland, G. J., 1980: An analytic model of the wind and pressure profiles in hurricanes. *Mon. Wea. Rev.,* **108,** 1212–1218.

——, J. I. Belanger, and A. Fritz, 2010: A revised model for radial profiles of hurricane winds. *Mon. Wea. Rev.,* **138,** 4393–4401.

Holmlund, K., C. Velden, and M. Rohn, 2001: Enhanced automated quality control applied to high-density satellite-derived winds. *Mon. Wea. Rev.,* **129,** 517–529.

Knaff, J. A., 2009: Revisiting the maximum intensity of recurving tropical cyclones. *Int. J. Climatol.,* **29,** 827–837.

——, and R. M. Zehr, 2007: Reexamination of tropical cyclone wind–pressure relationships. *Wea. Forecasting,* **22,** 71–88.

——, and B. A. Harper, 2010: Tropical cyclone surface wind structure and wind–pressure relationships. *Proc. Seventh Int. Workshop on Tropical Cyclones—VII,* La Reunion, France, WMO, 35 pp. [Available online at http://www.cawcr.gov.au/projects/iwtc/documentation/KN1.pdf.]

——, C. R. Sampson, M. DeMaria, T. P. Marchok, J. M. Gross, and C. J. McAdie, 2007: Statistical tropical cyclone wind radii prediction using climatology and persistence. *Wea. Forecasting,* **22,** 781–791.

——, D. P. Brown, J. Courtney, G. M. Gallina, and J. L. Beven II, 2010: An evaluation of Dvorak technique-based tropical cyclone intensity estimates. *Wea. Forecasting,* **25,** 1362–1379.

——, M. DeMaria, D. A. Molenar, C. R. Sampson, and M. G. Seybold, 2011: An automated, objective, multiple-satellite-platform tropical cyclone surface wind analysis. *J. Appl. Meteor. Climatol.,* **50,** 2149–2166.

Knapp, K. R., M. C. Kruk, D. H. Levinson, H. J. Diamond, and C. J. Neumann, 2010: The International Best Track Archive for Climate Stewardship (IBTrACS): Unifying tropical cyclone best-track data. *Bull. Amer. Meteor. Soc.,* **91,** 363–376.

Maclay, K. S., M. DeMaria, and T. H. Vonder Haar, 2008: Tropical cyclone inner-core kinetic energy evolution. *Mon. Wea. Rev.,* **136,** 4882–4898.

Merrill, R. T., 1984: A comparison of large and small tropical cyclones. *Mon. Wea. Rev.,* **112,** 1408–1418.

Mueller, K. J., M. DeMaria, J. Knaff, J. P. Kossin, and T. H. Vonder Haar, 2006: Objective estimation of tropical cyclone wind structure from infrared satellite data. *Wea. Forecasting,* **21,** 990–1005.

Neumann, C. J., 1993: Global overview. *Global Guide to Tropical Cyclone Forecasting,* G. J. Holland, Ed., WMO/TC-560, Rep. TCP-31, World Meteorological Organization, 1–43. [Available online at http://www.cawcr.gov.au/publications/BMRC_archive/tcguide/.]

Powell, M. D., S. H. Houston, L. R. Amat, and N. Morisseau-Leroy, 1998: The HRD real-time hurricane wind analysis system. *J. Wind Eng. Indust. Aerodyn.,* **77–78,** 53–64.

Rappaport, E. N., and Coauthors, 2009: Advances and challenges at the National Hurricane Center. *Wea. Forecasting,* **24,** 395–419.

Sampson, C. R., and A. J. Schrader, 2000: The Automated Tropical Cyclone Forecasting System (version 3.2). *Bull. Amer. Meteor. Soc.,* **81,** 1231–1240.

——, J. S. Goerss, and H. C. Weber, 2006: Operational performance of a new barotropic model (WBAR) in the western North Pacific basin. *Wea. Forecasting,* **21,** 656–662.

——, J. L. Franklin, J. A. Knaff, and M. DeMaria, 2008: Experiments with a simple tropical cyclone intensity consensus. *Wea. Forecasting,* **23,** 304–312.

Schwerdt, R. W., F. P. Ho, and R. R. Watkins, 1979: Meteorological criteria for standard project hurricane and probable maximum hurricane windfields, Gulf and East Coasts of the United States. NOAA Tech. Rep. NWS 23, 317 pp. [Available from National Hurricane Center Library, 11691 SW 117 St., Miami, FL 33165-2149.]

Velden, C. S., C. M. Hayden, S. J. Nieman, W. P. Menzel, S. Wanzong, and J. S. Goerss, 1997: Upper-tropospheric winds derived from geostationary satellite water vapor observations. *Bull. Amer. Meteor. Soc.,* **78,** 173–195.

Vickery, P. J., and D. Wadhera, 2008: Statistical models of Holland pressure profile parameter and radius to maximum winds of hurricanes from flight-level pressure and H*Wind data. *J. Appl. Meteor. Climatol.,* **47,** 2497–2517.

Willoughby, H. E., and M. E. Rahn, 2004: Parametric representation of the primary hurricane vortex. Part I: Observations and evaluation of the Holland (1980) model. *Mon. Wea. Rev.,* **132,** 3033–3048.